

FATIGUE AND SHEAR PROPERTIES OF HIGH RELIABLE SOLDER JOINTS FOR HARSH APPLICATIONS

Sinan Su¹, Minghong Jian¹, Francy John Akkara¹, Dr. Sa'd Hamasha¹, Dr. Jeff Suhling², Dr. Pradeep Lall²

¹Department of Industrial and Systems Engineering

²Department of Mechanical Engineering

Auburn University

AL, USA

smh0083@auburn.edu

ABSTRACT

The reliability of an electronic product in harsh applications is typically limited by the fatigue failure of one of the interconnected solder joints. Mechanical properties of common lead-free solder joints have been studied for large bulk solder samples. However, the microstructure of solder joints in a realistic application has been proved completely different than that of bulk solder samples, which can lead to different mechanical properties. SnAgCu (SAC) based solder alloys are widely used in the lead -free applications, however, solder alloys with only Sn, Ag and Cu demonstrate low reliability in harsh environments. In this study, individual high-reliability SnAgCu based solder joints (Innot, MaxRel, Ecolloy) were tested to investigate their shear and fatigue properties. The experiment includes shear of individual solder joints under 4 strain rates: 1, 0.1, 0.01, 0.001 sec⁻¹, and fatigue of individual solder joints under various stress amplitudes. For the shear testing, shear strengths of solder joints for each strain rate were systematically recorded and compared. For the fatigue testing, the effect of stress amplitude on the fatigue life and work dissipation was studied as well. Moreover, the effect of surface finish (OSP, ImAg, and ENIG) on the solder joints reliability was also investigated. The experiment results showed that shear strength tends to increase with the increase of shear strain rate. Solder joints with high Bi and Ag contents demonstrate superior shear and fatigue properties. However, excessive Bi may lead to the embrittlement of solder joints and change of failure modes during mechanical testing.

Key words: Solder joint, Reliability, Fatigue, Shear, Surface Finish

INTRODUCTION

The reliability of an electronic product in harsh applications is typically limited by the fatigue failure of one of the interconnected solder joints. SnAgCu (SAC) based solder alloys are widely used in the lead -free applications, however, solder alloys with only Sn, Ag and Cu demonstrate low reliability in harsh environments. In order to develop new lead-free solder alloys with better reliability, amounts of rare earth (RE) elements were selected as dopants into SAC based solder[1, 2]. Among them, Bismuth (Bi) doped SAC solder joints have shown several excellent mechanical properties in terms of tensile,

creep, or low cycle fatigue properties, and were viewed as a better candidate for harsh environment application. However, most of the mechanical properties testings were conducted using bulk sample, the microstructure of which has been proved completely different than solder joints in a realistic application [3-11]. In this study, three kinds of individual solder joints with "higher" Bi content (>2%) were selected, shear and fatigue properties were tested and investigated. Moreover, the effects of surface finish (OSP, ImAg, and ENIG) in combination with solder alloy selection on the reliability of solder joints were examined as well.

EXPERIMENTAL PROCEDURE

Test Vehicle and Sample Preparation

Solder joints investigated in this study are listed in table 1. All the solder joints were prepared of pure metals first and then soldered to Cu pads of testing vehicle during reflow process. Reflow was conducted in a nitrogen ambient with a peak temperature of 245°C and 45-60s above liquidus. A customized designed testing vehicle is shown in Figure 1. It consists of a FR4 glass-epoxy PCB and the dimensions of single testing board are 10mm X 10mm X 1mm, with 3mm pitch size. The diameter of a solder ball is 30mil. Solder-Mask-Defined (SMD) pads were used. Test vehicle with three surface finishes were used: OSP, ImAg and ENIG.

Table 1. Solder joints compositions

Materials	Compositions	Surface Finish
Innot	90.58Sn-3.5Ag-0.7Cu-3Bi-1.5Sb-0.125Ni	OSP, ImAg, ENIG
CycloMax	92.77Sn-3.41Ag-0.52Cu-3.3Bi	OSP, ImAg, ENIG
Ecolloy	96.62Sn-0.92Cu-2.46Bi	OSP, ImAg, ENIG

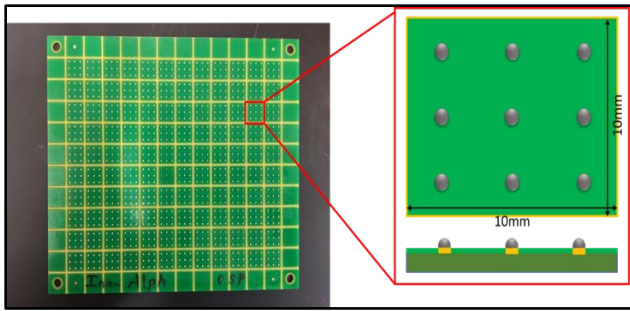


Figure 1. Test vehicle

Mechanical Testing Profile

Shear and low-cycle fatigue testing were conducted using a high accuracy Instron 5948 Micro-mechanical testing system with a special design fixture shown in Figure 2a. The system provides an axial displacement resolution of less than 10nm using preloaded ballscrews drive system, and a universal 50N load cell is utilized to simultaneously monitor forces and displacement. Shear testing is to investigate the integrity of individual solder joints within different solder materials with various surface finishes. Maximal shear strength (peak shear force over the cross-section area of solder joint) were recorded to test the shear properties of materials. The shear testing schematic is shown in Figure 2b. Shear properties of solder joints were achieved by setting the shear height of 0.05mm, and testing procedure is based on the JESD22-B117 shear testing standard. Solder ball shear testing was conducted at 4 different shear speeds: 0.33, 0.033, 0.0033, and 0.00033mm/s (1, 0.1, 0.01, and 0.001sec⁻¹) at ambient temperature. For each type of solder material, 10 samples were tested per stain rate, and total number of 120 samples were tested for the shear testing.

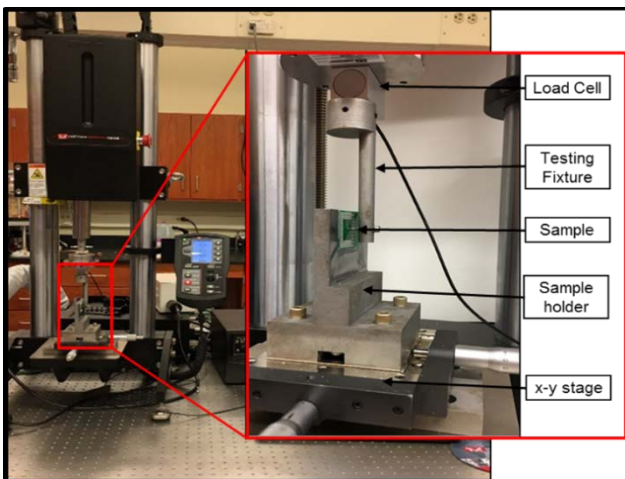


Figure 2a. Experimental setup

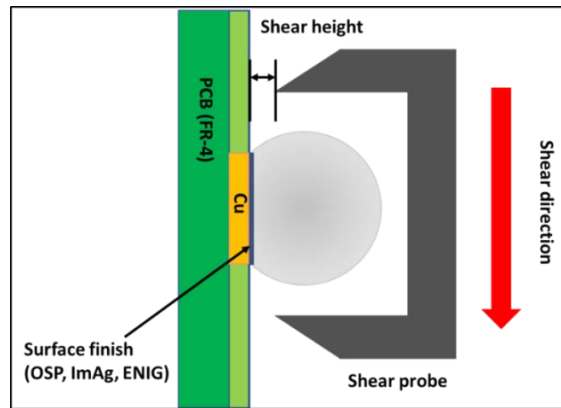


Figure 2b. Shear testing schematic

In terms of the low-cycle fatigue testing, the same Instron machine with fixture were used to perform a cyclic shear testing in this work. Fatigue failure of individual solder joint is defined as the time a sharp drop of stress-strain curve is detected during the cyclic shear testing. Fatigue life of individual solder joint under given stress amplitude is defined as the number of cycles until the fatigue failure of the solder joint [10]. By applying cyclic shear fatigue testing on individual solder joint, we can not only study the effect of solder alloy selection but the effect of intermetallic compound (IMC) and surface finish on the reliability of solder joint under low-cycle fatigue testing [12, 13], which not many researches have ever done that. In this study, solder joint was subjected to cyclic shear loading (stress controlled) at a constant strain rate $\dot{\epsilon} = 0.01 \text{ sec}^{-1}$. The shear probe moved downward first until it contacted the individual solder joint that was set up earlier inside the shear probe. The shear motion continued until the peak stress amplitude reached. Then the shear probe reversed its moving direction until the same stress amplitude was applied on the opposite of solder joint. Based on the different shear capacity of solder alloys and surface finish, 4 stress amplitudes from 16MPa to 32MPa were selected to ensure the fatigue life of each test is in a reasonable range. In addition, at least 7 tests were conducted per stress amplitude and a total number of 100 tests were finished.

RESULTS OF THE DATA

Effect of Surface Finish on Shear Strength

Shear strength of Ecolloy, Innolot and CycloMax solder alloy were plotted as a function of shear strain rate for three surface finishes as shown in Figure 3a, 3b, 3c. Shear strength (τ) can be expressed in terms of applied shear strain rate ($\dot{\gamma}$) in an approximately power equation [14]:

$$\tau = a [\ln(\dot{\gamma})]^b \dots\dots\dots(1)$$
 where a and b are material constants.

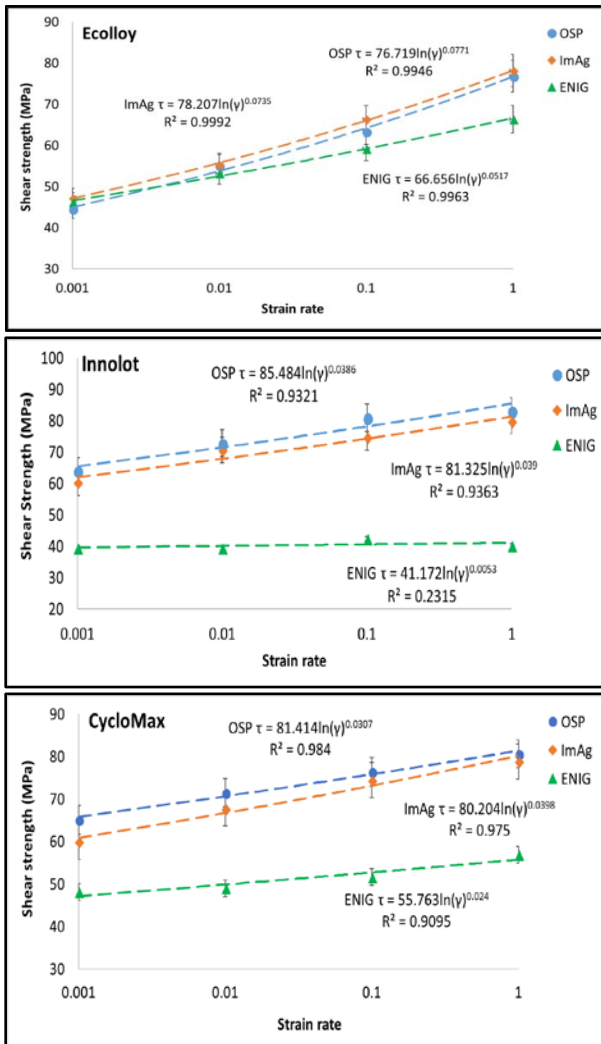


Figure 3. Shear strength vs. strain rate for (a) Ecolloy (b) Innolot (c) CycloMax solder alloys

It can be seen from Figure 3a, 3b, 3c, for solder alloys with OSP and ImAg surface finish, shear strength increases with the increase of strain rate. An average of 73% and 65% shear strength increase were observed from the slowest shear strain rate to the fastest shear strain rate (0.001 sec^{-1} to 1 sec^{-1}) for Ecolloy OSP and ImAg surface finish, respectively. In addition, 24% and 32% shear strength increase were seen for CycloMax OSP and ImAg surface finish, respectively, and 30% and 32% shear strength increase for Innolot OSP and ImAg surface finish, respectively. Shear strength of Ecolloy ENIG surface finish increase with the increase of shear strain rate by 43%, however, for Innolot and Ecolloy ENIG surface finish, shear strength is significantly lower than the OSP and ImAg surface finish, and no significant increment was seen with the increment of shear strength. Figure 4 further expounded this phenomenon. Bar chart on the left is shear strength companions for three solder alloys sheared under lower strain rate ($\dot{\gamma} = 0.001 \text{ sec}^{-1}$). In this figure, shear strength of OSP and ImAg surface finish of Innolot and CycloMax solder alloys exceeds that of Ecolloy by 46% and 27%, respectively. For ENIG surface finish, the differences among three solder materials are less. Bar chart on the right is shear strength comparisons for solder alloys under higher strain rate ($\dot{\gamma} = 1 \text{ sec}^{-1}$). In this figure, shear strength of OSP and ImAg surface finish of Ecolloy

caught up those of Innolot and CycloMax, and for ENIG surface finish, shear strength of Innolot and CycloMax were further decreased and Ecolloy turned out to be the highest.

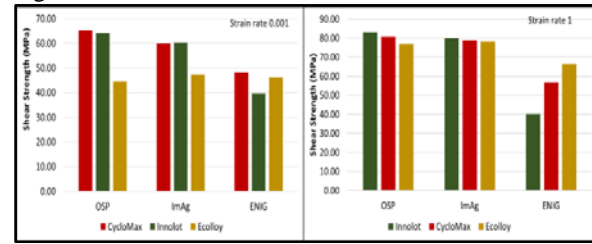


Figure 4. Solder materials shear strength comparisons at low/high strain rate

Fracture interfaces of solder joints with various surface finishes were shown in Figure 5 for shear testing with various solder alloys. Representative images are shown for the two failure modes that were detected in this test (brittle failure and ductile failure). Since SMD was applied on the testing board, no pad lifting failure was observed in this study.

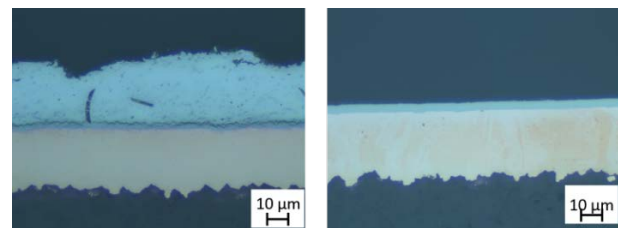


Figure 5. Failure modes observed: left: ductile failure; right: brittle failure

Besides images of fracture interfaces after shear testing, shear stress-strain curves were illustrated for both ductile and brittle failures in figure 6. In contrast to the ductile failure where stress-strain curve went through elastic and plastic deformation, then gradually decreased and finally fractured after ultimate shear stress: τ_{UTS} , brittle failure occurs prior to shear tool travelling the entire process [15]. Shear strength of brittle failure is only about 73% of that of ductile failure for the solder alloy exhibited, however, the integrated stress-strain curve area (fracture energy) of ductile failure could be many times greater than that of brittle failure [15].

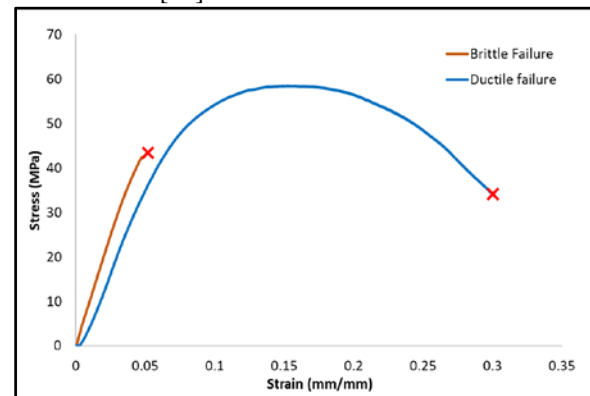


Figure 6. Typical stress-strain curve of ductile vs. brittle failure modes

After failure modes analysis for both fracture interfaces and failure curves, Innolot and CycloMax solder joints

with ENIG surface finish were demonstrated as brittle failure for all the shear strain rate ($\dot{\gamma} = 0.001, 0.01, 0.1, 1\text{sec}^{-1}$); Innolot and CycloMax solder joints with OSP and ImAg surface finishes were demonstrated as near brittle failure at high strain rate ($\dot{\gamma} = 1\text{sec}^{-1}$), and pure ductile failure for the rest of strain rates. Ecolloy were demonstrate as ductile failure at all strain rates. Combined with ductile and brittle failure curves, we concluded that the reason why shear strength for Innolot and CycloMax with ENIG is significantly lower than those of OSP and ImAg surface finishes is due to the transformation in failure modes between surface finishes. Since shear strength exhibited in brittle failure is lower than that in ductile failure, a clear drop in shear strength would be expected when switching from OSP or ImAg surface finish (ductile failure) to ENIG surface finish (brittle failure). Moreover, with abundant Ag and Bi in solder alloys (Innolot, CycloMax), the strength of them is enhanced. Fine grain strengthening of the microstructure and second phase strengthening of IMC were considered to be the major contributor to the increasement of bulk

strength [16, 17]. However, the existence of Bi and Ag would also increase the risk of brittleness of bulk solder and the chances for the appearance of brittle failure to the solder joints. For ENIG surface finish, several researches have pointed out that during shear testing, ENIG joint fractures along the interface, exhibiting a possibility brittle failure due to the embrittle of IMC layer [18, 19].

Effect of Surface Finish on Cyclic Fatigue Life

A two-parameter Weibull distribution was conducted to characterize the fatigue life of three lead-free solder joints with two surface finishes, as shown in figure 7a, 7b, 7c. A two-parameter Weibull distribution is expressed in equation 2:

$$\lambda(t) = \frac{\beta}{\theta} \left(\frac{t}{\theta}\right)^{\beta-1} \dots\dots\dots(2)$$

where β is shape parameter and θ is scale parameter. In this study, we take the scale parameter as the characteristic life which is the number of cycles at 63.2% of overall population to fail.

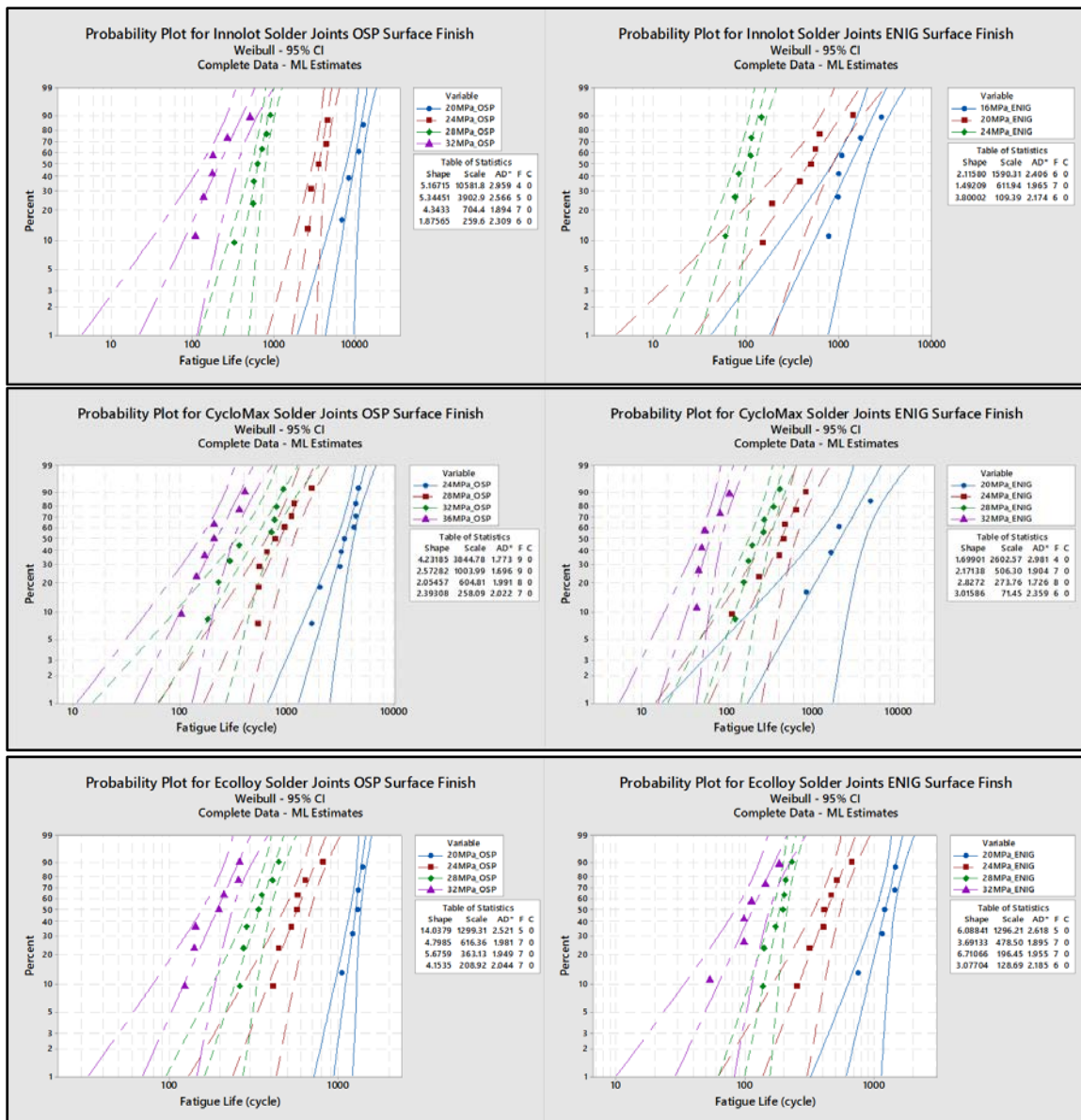


Figure 7. Weibull distribution for (a) Innolot (b) CycloMax (c) Ecolloy solder alloys with 2 surface finishes under 4 stress amplitudes

Characteristic fatigue life was plotted as a function of stress amplitudes in a log-log scale. Figure 8 shows an example of characteristic fatigue life vs. stress amplitude for Ecolloy OSP surface finish. A power equation was applied to fit the characteristic fatigue life (N_{63}) in terms of stress amplitudes (P) that applied on the solder joints during fatigue testing:

$$N_{63} = aP^{-c} \dots\dots\dots(3)$$

Where a and c are material constants. The absolute value of power value (c) represents the ductility of testing material. Smaller the power value, the larger the material ductility [12].

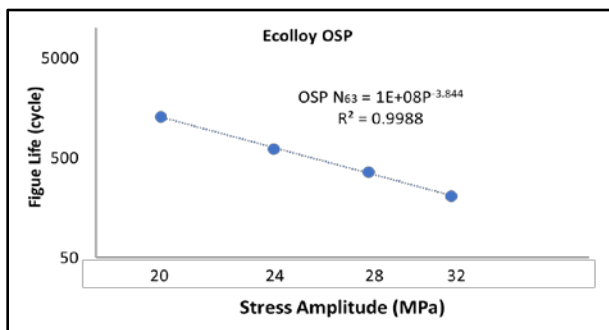


Figure 8. Example of fatigue life vs. stress amplitude for Ecolloy OSP

Figure 9a, 9b, 9c show fatigue life vs. stress amplitudes for Innolot, CycloMax and Ecolloy with OSP and ENIG surface finishes. In those figures we can find, all data points fit the power equation with R^2 larger than 0.97, which represents an excellent goodness-of-fit. Characteristic fatigue life associated with OSP surface finish was observed larger than that with ENIG surface finish for all the three solder materials, except that fatigue life differences between OSP and ENIG surface finishes are larger for Innolot and CycloMax than that of Ecolloy. Moreover, the regression lines for both surface finishes of single solder material are nearly parallel, demonstrates a similarity of power value, thus a similarity of material ductility, which indicates neither stress amplitude nor surface finish could influence the solder material ductility. The average absolute power values of Innolot, CycloMax, and Ecolloy are 7.341, 6.841, and 4.355, respectively, which indicates Ecolloy has higher ductility than Innolot and CycloMax. Figure 10 shows a fatigue life comparison for three solder materials cyclic sheared under 24MPa stress amplitude. Both CycloMax and Innolot show much higher fatigue life than that of Ecolloy for OSP surface finish, however, fatigue life was greatly decreased when being switched to ENIG surface finish. The joint effect of Ag and Bi would harden the solder material and enhance the fatigue resistance, at the expense of material ductility.

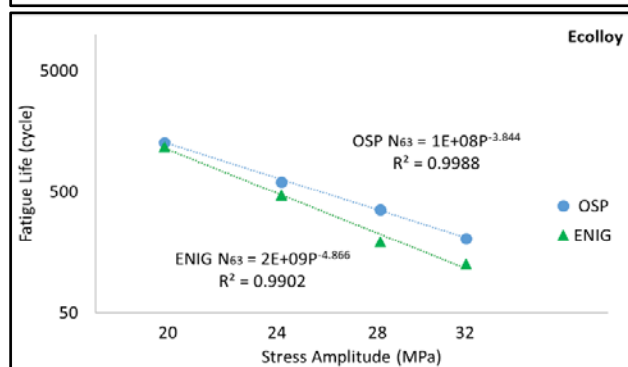
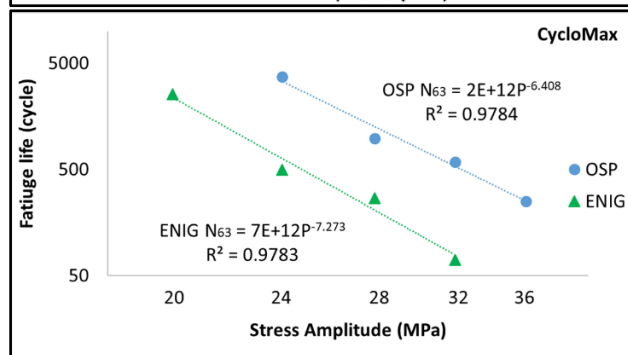
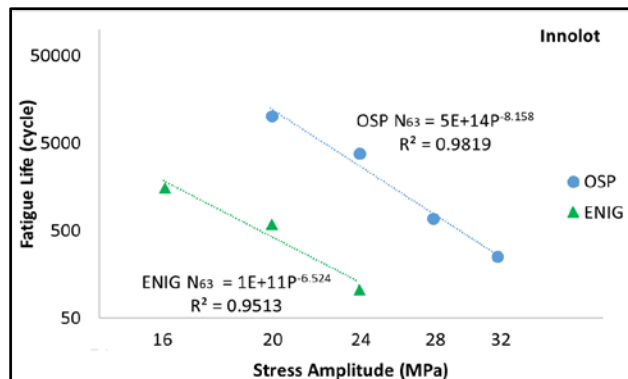


Figure 9. Fatigue life vs. stress amplitudes for 2 surface finishes for (a) Innolot (b) CycloMax (c) Ecolloy

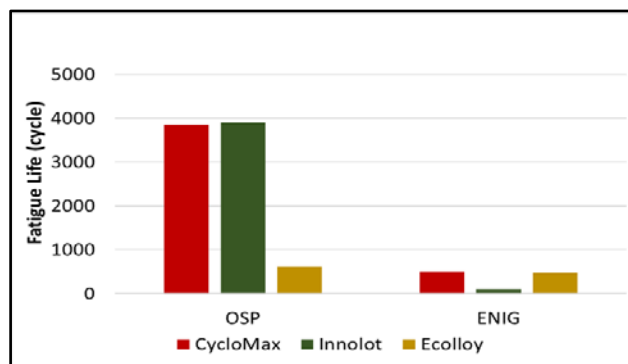


Figure 10. Fatigue life comparisons for 3 solder alloys at 24MPa

Effect of Solder Alloys on Cyclic Fatigue Hysteresis Loop

A typical hysteresis loop (cyclic stress-strain curve) for stress-controlled shear fatigue testing was shown in figure 11. A one degree-two parameter-linear model was used to fit the upper and lower half of experimental stress-strain curve separately. Take upper half of hysteresis loop for example, $f_1(\epsilon)$ represents the tension loading region and $f_2(\epsilon)$ represents the compression loading region [20]:

$$\begin{aligned} f_1(\epsilon) &= A_1 * \epsilon + B_1 \\ f_2(\epsilon) &= -A_2 * \epsilon + B_2 \dots\dots\dots(4) \end{aligned}$$

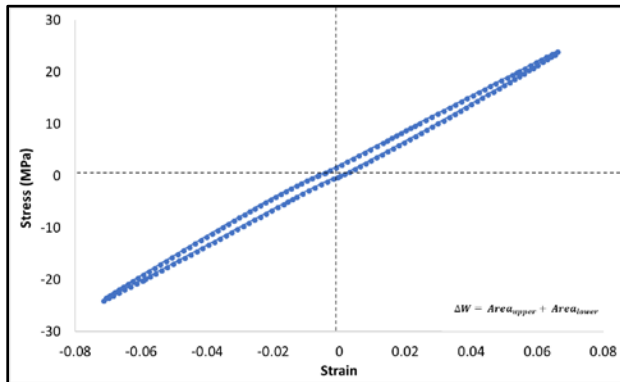


Figure 11. Typical hysteresis loop and area calculation

Hysteresis loop area for the upper half was calculated as the numerical integration between the two fitting equations. Hysteresis loop area for the lower half can be calculated using the same method. The whole hysteresis loop area is the sum of lower half area and upper half area, which represents the energy density dissipated per cycle during the cyclic loading. In the following hysteresis loop comparisons and energy density calculation, we would only represent the upper half of the hysteresis loop.

Figure 12 presented hysteresis loop comparisons for three solder alloys with OSP and ENIG surface finishes. Take 24MPa stress amplitude as an example, Ecolloy has the largest hysteresis loop than CycloMax or Innolot for both OSP and ENIG surface finish, since the ductility of Ecolloy is larger than them.

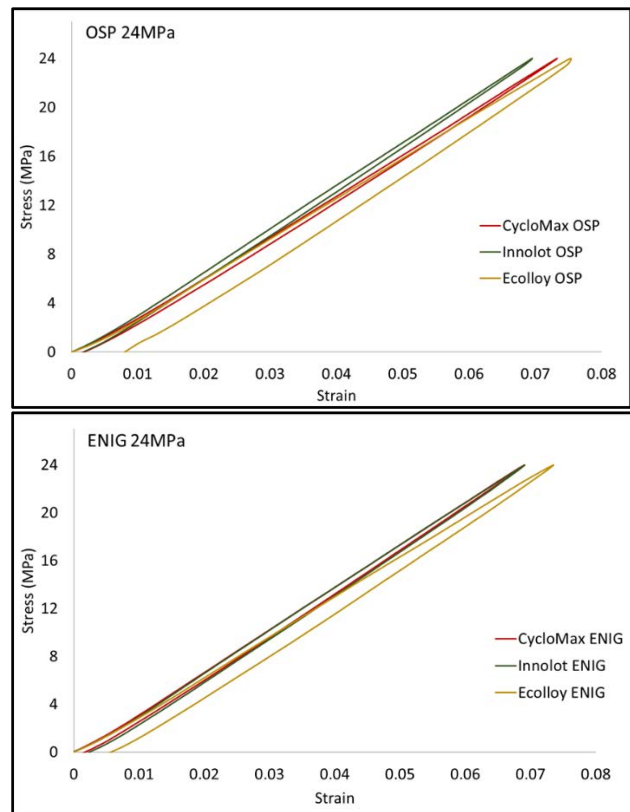


Figure 12. Hysteresis loop comparisons of 3 solder alloys under OSP and ENIG surface finishes at 24MPa

CONCLUSION

This study investigated the effect of surface finish and solder alloy on ball shear and cyclic fatigue testing. The results are summarized as follow:

- 1) Without considering the effect of surface finish, shear strength increases with the increasing shear strain rates. Fatigue life decreases with the increase of stress amplitudes.
- 2) Brittle failure was observed for ENIG surface finish at all shear strain rate, for both Innolot and CycloMax solder joints. Solder joints with OSP and ImAg surface finish are prone to ductile failure during shear testing.
- 3) Solder joints with high Ag and Bi content demonstrated better reliability in terms of shear and fatigue testing. Ag and Bi enhanced the strength of IMC particles in the solder, thus harden the solder bulk and increase the fatigue resistance.

ACKNOWLEDGEMENTS

This research was supported by Gradated NSF Center for Advanced Vehicle and Extreme Environment Electronics (CAVE3) at Auburn University

REFERENCES:

- [1] C. Zhao, T. Sanders, Z. Hai, C. Shen, and J. L. Evans, "Reliability Analysis of Lead-Free Solder Joints with Solder Doping on Harsh Environment," in *International Symposium on Microelectronics*, 2016, pp. 000117-000122.
- [2] C. Zhao, T. Sanders, C. Shen, Z. Hai, J. L. Evans, M. Bozack, *et al.*, "RELIABILITY OF DOPED LEAD-FREE SOLDER JOINTS UNDER ISOTHERMAL AGING AND THERMAL CYCLING."
- [3] P. Borgesen, S. Hamasha, M. Obaidat, V. Raghavan, X. Dai, M. Meilunas, *et al.*, "Solder joint reliability under realistic service conditions," *Microelectronics Reliability*, vol. 53, pp. 1587-1591, 2013.
- [4] P. Borgesen, S. Hamasha, L. Wentlent, D. Watson, and C. Greene, "Interpreting accelerated test results for lead free solder joints," in *Pan Pacific Microelectronics Symposium (Pan Pacific)*, 2016, 2016, pp. 1-9.
- [5] S. Hamasha and P. Borgesen, "Effects of Strain Rate and Amplitude Variations on Solder Joint Fatigue Life in Isothermal Cycling," *Journal of Electronic Packaging*, vol. 138, p. 021002, 2016.
- [6] S. Hamasha, Y. Jaradat, A. Qasaimeh, M. Obaidat, and P. Borgesen, "Assessment of Solder Joint Fatigue Life Under Realistic Service Conditions," *Journal of electronic materials*, vol. 43, 2014.
- [7] S. Hamasha, A. Qasaimeh, Y. Jaradat, and P. Borgesen, "Correlation between solder joint fatigue life and accumulated work in isothermal cycling," *IEEE Transactions on Components, Packaging and Manufacturing Technology*, vol. 5, pp. 1292-1299, 2015.
- [8] S. Hamasha, S. Su, F. Akkara, A. Dawahdeh, P. Borgesen, and A. Qasaimeh, "Solder joint reliability in isothermal varying load cycling," in *Thermal and Thermomechanical Phenomena in Electronic Systems (ITherm)*, 2017 16th IEEE Intersociety Conference on, 2017, pp. 1331-1336.
- [9] S. Hamasha, L. Wentlent, and P. Borgesen, "Statistical Variations of Solder Joint Fatigue Life Under Realistic Service Conditions," *IEEE Transactions on Components, Packaging and Manufacturing Technology*, vol. 5, pp. 1284-1291, 2015.
- [10] A. Qasaimeh, S. Hamasha, Y. Jaradat, and P. Borgesen, "Damage evolution in lead free solder joints in isothermal fatigue," *Journal of Electronic Packaging*, vol. 137, p. 021012, 2015.
- [11] L. Wentlent and P. Borgesen, "Statistical Variations of Solder Joint Fatigue Life Under Realistic Service Conditions," *IEEE Transactions on Components, Packaging and Manufacturing Technology*, vol. 5, pp. 1284-1291, 2015.
- [12] S. Su, N. Fu, F. J. Akkara, and S. Hamasha, "Effect of Long-Term Room Temperature Aging on the Fatigue Properties of SnAgCu Solder Joint," *Journal of Electronic Packaging*, vol. 140, p. 031005, 2018.
- [13] S. Hamasha, F. Akkara, S. Su, H. Ali, and P. Borgesen, "Effect of Cycling Amplitude Variations on SnAgCu Solder Joint Fatigue Life," *IEEE Transactions on Components, Packaging and Manufacturing Technology*, 2018.
- [14] J. Y. H. Chia, B. Cotterell, and T. C. Chai, "The mechanics of the solder ball shear test and the effect of shear rate," *Materials Science and Engineering: A*, vol. 417, pp. 259-274, 2006.
- [15] F. Song, S. R. Lee, K. Newman, B. Sykes, and S. Clark, "Brittle failure mechanism of SnAgCu and SnPb solder balls during high speed ball shear and cold ball pull tests," in *Electronic Components and Technology Conference, 2007. ECTC'07. Proceedings. 57th*, 2007, pp. 364-372.
- [16] Y. Liu, F. Sun, and X. Li, "Effect of Ni, Bi concentration on the microstructure and shear behavior of low-Ag SAC-Bi-Ni/Cu solder joints," *Journal of Materials Science: Materials in Electronics*, vol. 25, pp. 2627-2633, 2014.
- [17] C. Zhao, "Board Level Reliability of Lead-Free Solder Interconnections with Solder Doping Under Harsh Environment," 2017.
- [18] M. Alam, Y. Chan, and K. Tu, "Elimination of Au-embrittlement in solder joints on Au/Ni metallization," *Journal of materials Research*, vol. 19, pp. 1303-1306, 2004.
- [19] J.-W. Yoon, B.-I. Noh, and S.-B. Jung, "Comparative study of ENIG and ENEPIG as surface finishes for a Sn-Ag-Cu solder joint," *Journal of electronic materials*, vol. 40, pp. 1950-1955, 2011.
- [20] N. Fu, J. C. Suhling, S. Hamasha, and P. Lall, "Evolution of the cyclic stress-strain and constitutive behaviors of SAC305 lead free solder during fatigue testing," in *Thermal and Thermomechanical Phenomena in Electronic Systems (ITherm)*, 2017 16th IEEE Intersociety Conference on, 2017, pp. 1353-1360.